RESEARCH PAPER

Rational Design and Synthesis of Covalent KRASG12C Inhibitors as Potential Anticancer Agents

Lala S. Rathod[1], Santosh N. Mokale[2], Vinod Mokale[1]*

[1]University Department of Pharmaceutical Sciences, MGM University, N-6, CIDCO, MGM Campus, Chhatrapati Sambhajinagar (Aurangabad)- 431003, Maharashtra, India

[2]Y. B. Chavan College of Pharmacy, Chhatrapati Sambhajinagar (Aurangabad)- 431001, Maharashtra, India

***Corresponding author: Vinod Mokale**

Email: mokalevinod@gmail.com | Orchid ID: 0000-0003-3661-6395

Received: 21st Feb, 2026; Revised: 8th April, 2026; Accepted: 11th May, 2026; Available Online: 12th June, 2026

Lala S. Rathod Email: lalarathod@gmail.com | Orchid ID: 0000-0002-9412-2900

Santosh N. Mokale Email: santoshmokale@gmail.com | Orchid ID: 0000-0002-9860-8895

ABSTRACT

The presence of KRAS mutations is one of the most common reasons of oncogenic transformation of human cells. In particular, the KRASG12C mutation is observed quite often in non-small cell lung cancer, colorectal cancer, and pancreatic cancer. The substitution of glycine for cysteine at position 12 results in the creation of a specific nucleophile residue which provides possibilities for selective and irreversible targeting, thus, allowing for precision oncology. In this work, a novel series of covalent KRASG12C inhibitors was designed on the basis of a rational structure-based approach aimed at the inhibition of inactive G-DP bound mutant KRASG12C protein in the allosteric switch-II pocket.

The synthesized molecules were characterized by standard methods and then tested for anticancer activity both in silico and in vitro. In particular, molecular docking experiments showed proper binding to key residues of the switch-II pocket and covalent attachment to the Cys12 residue of mutant KRASG12C protein. Moreover, cytotoxic activity against various KRAS-mutant cancer cell lines was determined in order to estimate the ability of the synthesized molecules to disrupt KRAS-mediated downstream signaling pathways.

This study demonstrates the value of using rational design approaches to generate selective KRASG12C inhibitors through covalent binding, and also sheds some light on SARs that could assist future optimization of these agents.

Keywords: KRASG12C Mutation, Covalent Inhibitors, Structure-Based Drug Design, Molecular Docking, Targeted Anticancer Therapy.

How to cite this article: Rathod LS, Mokale SN, Mokale V. Rational Design and Synthesis of Covalent KRASG12C Inhibitors as Potential Anticancer Agents. Int J Drug Deliv Technol. 2026;16(59s): 7-13. DOI: 10.25258/ijddt.16.59s.2

Source of support: Nil

Conflict of interest: None

Introduction:

It is still one of the biggest diseases across the globe and accounts for a large portion of global deaths even after the advent of several effective methods for its detection and treatment. The development and progression of cancer involves many genetic and epigenetic changes that affect cellular pathways and lead to uncontrolled cell growth, therapeutic resistance, apoptosis resistance, and enhanced cell invasion. Among other oncogenic pathways identified in carcinogenesis, the mutation of RAS family of proto-oncogenes has gained much importance because of their high frequency of occurrence and significance in regulating cell signaling pathways[1].

RAS family has three similar members; the HRAS, NRAS, and KRAS. They encode small guanosine triphosphatases that act as regulators of intracellular signaling pathway. These are considered as molecular switches that change from their inactive state when bound to guanosine diphosphate (GDP) to an active form when they are attached to guanosine triphosphate (GTP). In normal biological conditions, activation of RAS is regulated through interaction with guanine nucleotide exchange factors (GEFs) like SOS family proteins and GTPase-activating proteins (GAPs). This helps in maintaining signaling balance. Mutations in RAS proteins affect the signaling regulation process and lead to the permanent activation of the signal pathway. The KRAS isoform is the most common type of RAS mutation that causes cancer and is seen in nearly 85% cases of RAS-driven cancers. KRAS mutations can be seen in NSCLC, PDAC, CRC, and other solid malignancies. Inactivation of KRAS results from mutations at codons 12, 13, and 61, affecting GTP hydrolysis, leading to persistent activation of the RAF–MEK–ERK and PI3K–AKT–mTOR signaling pathways. Activation of these signaling pathways leads to initiation, progression, angiogenesis, and metastasis, among others, and confers resistance to standard therapy[2],[3]. Out of different KRAS mutations, KRASG12C mutation holds a particular significance as a potential therapeutic target. In this case, there is an exchange between the amino acids glycine and cysteine in codon 12 of KRAS gene,

which results in the generation of a unique nucleophile. KRASG12C mutation is prevalent in cases of lung adenocarcinoma but it is also seen in some other forms of cancer such as colorectal and pancreatic cancers. Presence of cysteine at codon 12 gives an exclusive chance of selective covalent modification that cannot occur in case of wild-type KRAS[2].

For many years, KRAS remained to be an "undruggable" target due to multiple constraints including structural and biochemical aspects. Firstly, the protein surface of KRAS is almost smooth in nature without any deep pockets for binding by a small molecule. Secondly, KRAS is extremely sensitive toward GDP and GTP, having picomolar affinity toward these molecules, so its inhibition is very difficult. For this reason, drug development for many years proved unsuccessful but then things changed through the identification of an allosteric pocket named Switch-II pocket (S-IIP)[4]. The presence of the switch-II pocket proved to be a groundbreaking moment in KRAS drug discovery. It is available mainly in the inactive form of KRASG12C protein and allows targeting KRAS with selectivity using a small-molecule approach. Specifically, covalent inhibitors that bind to the switch-II pocket can use their electrophilic warheads to establish permanent bonds with the mutant cysteine group. In turn, this covalent interaction ensures that KRAS remains inactive and unable to transmit any signal further, resulting in cell growth inhibition[2,5].

As a result, covalent inhibition has become a promising method in contemporary medicinal chemistry since it offers a number of benefits, such as increased selectivity, target residence time, and more powerful pharmacodynamics. In KRASG12C drug design, it is essential to use electrophiles to ensure the reaction between Cys12 residue of KRAS and the drug. As for structural modifications of such inhibitors, their efficacy depends on the proper placement of electrophile moieties and optimal hydrophobic interactions[6].

The past few years have seen tremendous success in KRASG12C targeted therapy through the approval of several drugs specifically for this mutation. These molecules proved KRASG12C as a druggable and actionable oncogenic driver and set up a new standard for precision oncology. Despite these successes, however, several limitations still need to be overcome[7]. One major issue that arises is clinical resistance due to secondary mutations, pathway reactivation, bypass signaling pathways, and adaptive responses in cells. In addition, limited duration of response and efficacy variability among different tumor types make it necessary to explore other structural classes of inhibitors[8].

The development of modern tools of computational chemistry, molecular docking, structure-based drug design, and medicinal chemistry contributed significantly to the rapid discovery of new KRAS inhibitors[9]. Drug design strategies allow the creation of new chemical structures that can interact more effectively with the switch-II pocket but will possess good physical and pharmacological properties at the same time[8].

Materials and methods

Chemistry

The chemicals and reagents used in this experiment were supplied by Merck Life Science Pvt Ltd., BLD Pharm Limited, Sigma-Ald□rich, Avra Synthesis Private Ltd., and Molychem and were used in pure forms. Silica gel precoated aluminum TLC plates obtained from Sigma-Aldrich (Silica gel 60 F254) were used to check the progress of the reactions while an indicator like Iodine vapor or UV radiation was used to visualize the results. Finar 200-400 mesh silica gel was used for column and flash chromatography (Automated Yamazen Flash Chromatography). Melting points (uncorrected) were measured using the OptiMelt MPA100 melting point apparatus. Mass Spectra (MS) were done using (Shimadzu LC-MS 8040 System). The 1H NMR and 13C NMR spectra were recorded on (Bruker, Innova Varian-VXR-Unity) 500 MHz and (JEOL, ECZR Series) 600 MHz NMR spectrometer. The splitting patterns used are singlet (s), doublet (d), triplet (t), and δ values were reported in parts per million (ppm) relative to the internal TMS standard.

General procedure for synthesis of ethyl 4-(4-acryloylpiperazin-1-yl)-7-(phenylsulfonyl)-7H-pyrrolo[2,3-d]pyrimidine-6-carboxylate and related analogs

Step-I

A solution of **4-chloro-1H-pyrazolo[3,4-d]pyrimidine** (1.04 mmol) in dry DMF was treated with **sodium hydride** (NaH) (60% dispersion in mineral oil) (2.35 mmol) under a nitrogen atmosphere and cooled in an ice bath and stirred for 15 min. The ice bath was then removed and stirring was continued for another 30 min at room temperature. After dropwise addition of a solution of **substituted benzyl chloride** (2.08 mmol) in dry DMF, the mixture was stirred at room temperature for 3 h. After addition of water, the reaction mixture was exhaustively extracted with ethyl acetate. The combined organic phases were washed with brine, dried over sodium sulfate, and concentrated under reduced pressure. The residue was purified by chromatography on silica gel (chloroform/methanol, 9: 1) to yield as a solid[10].

Step-2: 4-chloro-1-(substituted-benzyl)-1H-pyrazolo[3,4-d]pyrimidine (2 mmol) was added to a stirred mixture of **1-Boc-piperazine** 2.1 mmol) and DIPEA Add Slowly (6 mmol) in 2-Propanol (10 mL). The reaction mixture was stirred at 0°C for 2 hrs. Add 25-50 ml cold water in reaction mixture solid precipitate form filter and dried.

Step-3: TFA (2 mL) and DCM (2 mL) was added to **tert-butyl 4-(1-(substituted-benzyl)-1H-pyrazolo[3,4-d]pyrimidin-4-yl)piperazine-1-carboxylate** (6 mmol). The resulting mixture was stirred at room temperature for 1 h and then was concentrated.

Step-4: Acryloyl chloride (0.16 mmol) was added to a stirred mixture of **1-(substitutes-benzyl)-4-(piperazin-1-yl)-1H-pyrazolo[3,4-d]pyrimidine** (0.15 mmol) and triethylamine (0.44 mmol) in DCM (1 mL). The reaction mixture was stirred at rt for 30 min. The reaction mixture was quenched with saturated aqueous sodium bicarbonate (15 mL) and extracted with DCM (20 mL). The organic layer was separated, dried over MgSO4, filtered, and concentrated in vacuo [11,12,13]

1. 1-(4-(7-(2-chlorobenzyl)-7H-pyrrolo[2,3-d]pyrimidin-4-yl)piperazin-1-yl)prop-2-en-1-one 1-(4-(7-(2-chlorobenzyl)-7H-pyrrolo[2,3-d]pyrimidin-4-yl)piperazin-1-yl)prop-2-en-1-one **Chemical Formula**: $C_{20}H_{20}ClN_5O$ **Molecular Weight**: 381.86 found and Purified by flash chromatography (0%→80% Ethyl Acetate in Hexane); Off White Solid; Yield 78.29 %; mp 188-190°C

   ^{1}H NMR: δ **3.96-3.73** (8H, 3.96 (ddd, *J* = 14.3, 6.7, 2.8 Hz), 3.73 (ddd, *J* = 12.8, 6.7, 2.8 Hz)), **6.59-6.54** (2H, s), **5.78** (1H, dd, *J* = 10.9, 1.5 Hz), **6.38** (1H, dd, *J* = 17.0, 1.5 Hz), **7.30-7.27** (2H, **7.30** (dd, *J* = 17.0, 10.9 Hz), **7.27** (ddd, *J* = 8.1, 1.6, 0.5 Hz)), **7.53-7.52** (2H, 7.20 (ddd, *J* = 7.53, 7.5, 1.6 Hz), 7.27 (ddd, *J* = 8.3, 7.5, 1.6 Hz)), **7.47** (1H, ddd, *J* = 8.3, 1.6, 0.5 Hz), **8.07** (1H, s), **8.43** (1H, s).

   13C NMR: δ 45.5-44.8 (3C, 45.5 (s), 44.8 (s)), 41.5 (2C, s), 77.3 (1C, s), 77.0 (1C, s), 76.6 (1C, s), 104.4 (1C, s), 105.0 (1C, s), 122.1 (1C, s), 126.9 (1C, s), 128.2 (1C, s), 128.8 (1C, s), 129.6 (1C, s), 145.5 (1C, s), 152.8 (1C, s), 156.8 (1C, s), 165.1 (1C, s).

2. 1-(4-(1-(2,6-difluorobenzyl)-1H-pyrazolo[3,4-d]pyrimidin-4-yl)piperazin-1-yl)prop-2-en-1-one **Chemical Formula**: $C_{19}H_{18}F_2N_6O$ **Molecular Weight:** 384.38 found & Purified by flash chromatography (0%→80% Ethyl Acetate in Hexane); Off White Solid; Yield 90.30 %; mp 170-172°C
3. 1-(4-(1-(2-(trifluoromethyl)benzyl)-1H-pyrazolo[3,4-d]pyrimidin-4-yl)piperazin-1-yl)prop-2-en-1-one **Chemical Formula:** $C_{20}H_{19}F_3N_6O$ **Molecular Weight:** 416.40 found & Purified by flash chromatography (0%→80% Ethyl Acetate in Hexane); White Solid; Yield 79.20 %; mp 183-185°C
4. 1-(4-(1-(4-chloro-2-fluorobenzyl)-1H-pyrazolo[3,4-d]pyrimidin-4-yl)piperazin-1-yl)prop-2-en-1-one **Chemical Formula:** $C_{19}H_{18}ClFN_6O$ **Molecular Weight**: 400.84 found & Purified by flash chromatography (0%→80% Ethyl Acetate in Hexane); White Solid; Yield 80.00 %; mp 187-190°C
5. 1-(4-(1-(2-fluorobenzyl)-1H-pyrazolo[3,4-d]pyrimidin-4-yl)piperazin-1-yl)prop-2-en-1-one **Chemical Formula**: $C_{19}H_{19}FN_6O$ **Molecular Weight**: 366.39 found & Purified by flash chromatography (0%→80% Ethyl Acetate in Hexane); off White Solid; Yield 80.00 %; mp 188-190°C

Results and Discussion

Molecular Docking Studies

The binding properties of the designed compounds and their comparative analysis with the reference inhibitor Sotorasib were determined based on molecular docking experiments. Docking was verified with the use of the co-crystallized structure of KRASG12C (PDB code: 6OIM) with standard molecules having characteristic binding properties with amino acids located in the switch-II pocket (S-IIP). This confirmed that our docking technique is appropriate for such analysis[14].

A study of the interaction properties of Sotorasib revealed an ideal location inside the KRASG12C active site by interacting with essential amino acids including Cys12, Gly13, Lys16, Tyr96, Gln99, Ile100, and Val103. The interaction with Cys12 residue is especially crucial because selectivity of mutant-specific KRASG12C inhibition requires specific binding of the molecule to this site. Moreover, interactions with hydrophobic amino acids like Tyr96, Ile100, and Val103 were responsible for the hydrophobic pocket stability[15].

It was noted that the binding positions of the synthesized analogs were similar to one another within the switch-II pocket, implying the capability of these compounds to enter the allosteric site and hinder the function of KRAS. Some structural changes in the synthesized analogs could have contributed to the change in binding interactions and increased binding efficiency in the switch-II pocket.

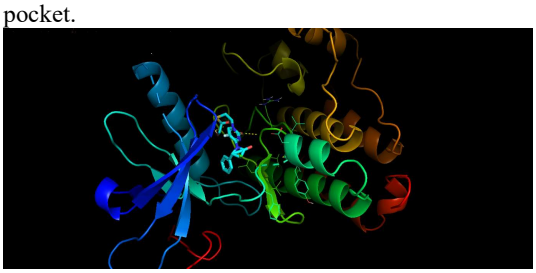

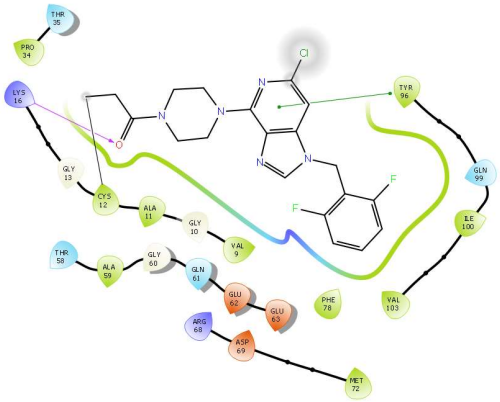

Figure: 1 Two-dimensional interaction diagram showing the binding interactions of the standard inhibitor Sotorasib within the active site of KRASG12C (PDB ID: 6OIM), highlighting key amino acid residues involved in switch-II pocket recognition and ligand stabilization.

Physicochemical Properties and ADME Evaluation

The physicochemical and pharmacokinetic properties of synthesized molecules were predicted through computational ADMET evaluation to determine the drug-like nature and oral bioavailability of the compounds. Molecular weights of the synthesized compounds were within the range of 348.40 – 417.29 g/mol, which are significantly low compared to the reference inhibitor Sotorasib at 560.59 g/mol. Low molecular weight usually indicates good permeability and pharmacokinetic properties.

Majority of the synthesized compounds had relatively similar TPSA values, which were mostly 67.15 Å2; however, Molecule 9 displayed high TPSA value at 76.38 Å2. All of the calculated values are within the acceptable range for oral drug candidates and display good membrane permeability. Lipophilicity evaluation produced iLOGP values between 2.10 – 3.35, which were lower than Sotorasib at 4.10, reflecting optimal hydrophobic-hydrophilic balance of the molecules. All the compounds had high gastrointestinal absorption and good bioavailability values of 0.55, showing potential oral drug properties. The majority of the compounds were found to have good solubility while compounds 3 and 9 showed moderate solubility levels. All the synthesized compounds complied with the Lipinski's rule of five without any violations as opposed to Sotorasib which had one violation. In addition, low synthetic accessibility scores of 2.79-3.02 demonstrated ease of synthesis when compared with Sotorasib (4.65). These results suggest that the analogues had better drug-like features compared to the reference compound.

Biological Activity Against KRASG12C Mutant NCI-H358 Cells

The compounds were tested for their inhibitory activity against the KRASG12C mutant in NCI-H358 cells using the IC50 assay. The heterogeneity of IC50 values among the analyzed compounds was observed, with the values lying between 2.38 µM and 16.18 µM.

According to the results obtained, the most potent molecules against NCI-H358 cells are Molecule 6 with an IC50 value of 2.38 µM, Molecule 2 with an IC50 value of 2.45 µM, Molecule 9 with an IC50 value of 2.46 µM, and Molecule 3 with an IC50 value of 2.50 µM. Such high potencies may result from the ability of these compounds to interact well with the target. As far as the moderate activity is concerned, Molecule 7 was identified with an IC50 value of 4.31 µM. Intermediate potencies of Molecule 4 (10.33 µM) and Molecule 8 (9.40 µM) were detected. Moreover, Molecule 1 and 5 demonstrated low antiproliferative potential (IC50 = 16.18 µM and 15.48 µM)[16].

The potency of the reference compound, Sotorasib, against NCI-H358 cells equals 32 nM. Even if the potency of the analogs is lower compared to that of the standard compound, their activity is quite promising and can be used for further modification[17].

Structure	Code	Derivatives	Activity IC_{50}	Docking Score
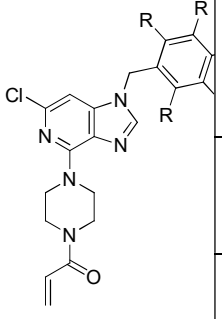	6	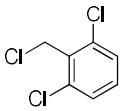	16.18	-7.6
	7	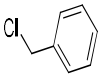	2.45	-6.9
	8	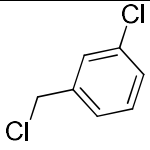	2.5	-6.7
	9	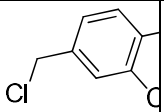	10.33	-7.3

	10	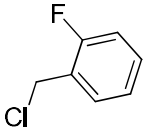	15.48	-6.7
	1	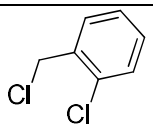	2.38	-7.3
	3	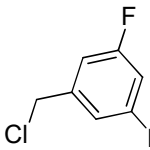	4.31	-6.0
	11	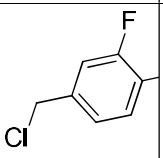	9.40	-7.0
	4	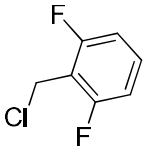	2.46	-6.0
	12	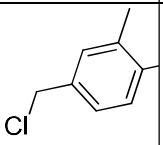	19.69	-7.3
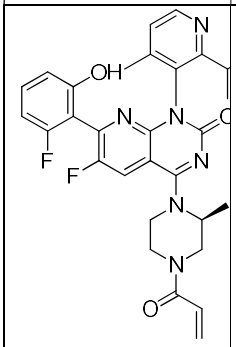	Standard	**Sotorasib**	32.25	-7.9

Table 1: IC_{50} Value & Docking Score

ADME

Based on comparisons of the bioactivity among the synthesized molecules, it appears that small differences in structures greatly affect the ability of a molecule to inhibit cancer proliferation. Compounds that exhibited high potency showed balanced lipophilicity, good prediction of solubility, and reduced molecular weights, potentially resulting in increased membrane permeation and binding affinity.Moreover, compounds with higher potency showed good docking properties at the switch-II site, hinting at the possibility that docking behavior could have an effect on the inhibition of proliferation. Overall, based on the SAR studies, it is likely that more refined design of substituents, hydrophobicity, and warhead covalent orientation can increase KRASG12C inhibitory activity.Taken together, all of these considerations show that the designed compounds have the necessary qualities to become effective drugs for cancer therapy.

Compound	**MW (g/mol)**	**HBA**	**HBD**	**RB**	**TPSA (Å²)**	**iLOGP**	**Solubility Class**	**GI Absorption**	**BBB Permeation**	**Lipinski Violations**	**Bioavailability Score**	**Synthetic Accessibility**
Molecule1	382.85	4	4	5	67.15	2.73	Soluble	High	Yes	0	0.55	2.86
Molecule2	384.38	5	6	5	67.15	2.3	Soluble	High	No	0	0.55	2.88
Molecule3	416.4	6	7	6	67.15	2.98	Moderately Soluble	High	No	0	0.55	3.02
Molec	400.	5	5	5	67.1	2.83	Solu	High	Yes	0	0.55	2.92

ule 4	84				5		ble				
Molecule 5	386.39	5	5	5	67.15	2.2	Soluble	High	Yes	0	0.55	2.86
Molecule 6	417.29	5	4	5	67.15	3.35	Soluble	High	No	0	0.55	2.89
Molecule 7	348.4	5	4	5	67.15	2.1	Soluble	High	No	0	0.55	2.79
Molecule 8	382.85	5	4	5	67.15	2.73	Soluble	High	Yes	0	0.55	2.85
Molecule 9	412.87	6	5	6	76.38	2.7	Moderately Soluble	High	—	—	0.55	—
Sotorasib (Standard)	**560.59**	—	—	—	**1044.45**	**4.1**	**Moderately Soluble**	**High**	**No**	**1**	**0.55**	**4.65**

Table: 2 ADME Evaluations

Conclusion

As shown by the findings of the current research work, a set of new KRASG12C covalent inhibitors was successfully rationalized, synthesized, and evaluated in terms of their potential anticancer activity on cancer models containing KRAS-mutant cells. In the course of computational screening of binding sites, docking experiments have revealed optimal binding poses of synthesized molecules inside the KRASG12C switch-II pocket with crucial interactions with essential residues.

According to the ADME analysis of the synthesized substances, favorable features include low molecular weight, proper lipophilicity, high predicted oral absorption rate, good bioavailability, and compliance with Lipinski's rule of five. Moreover, the synthesized analogues appeared to be less complex synthetically and had higher predicted drug likeness than the reference compound Sotorasib.

The biological evaluation of the molecules on KRASG12C mutant NCI-H358 cells revealed significant antiproliferative activity, where some molecules showed low micromolar IC50 values. In terms of structure-activity relationship studies, it was noted that Molecule 6 was the most potent molecule with an IC50 value of 2.38 µM, followed by Molecules 2, 9, and 3, implying that changes in chemical structures play an important role in the biological activity and interaction with targets. While comparing the biological results of molecules with that of the standard inhibitor Sotorasib, the molecules were less potent; however, the drug-like nature of the molecules reveals their potential as lead compounds.

In conclusion, the application of rational drug designing, molecular modeling, physiochemical analysis, and biological evaluation gives valuable information regarding the designing of the next-generation inhibitors for KRASG12C.

Acknowledgments

The authors are sincerely grateful to the University Department of Pharmaceutical Sciences, MGM University, Chhatrapati Sambhajinagar (Aurangabad)-431003, Maharashtra, India, for providing the necessary facilities and infrastructure to carry out this research work.

Authors Contribution:

Lala S. Rathod: writing – Original draft

Santosh N. Mokale: Conceptualization, Review & Editing

Vinod Mokale: Supervision, Review & Editing
All the authors critically revised and approved the final version of the manuscript

Ethics approval

None

Funding

None

Conflict of interest

The authors declare that they have no known competing financial interests or personal relationships that could have appeared to influence the work reported in this paper.

References:

1. Cox, A. D., Fesik, S. W., Kimmelman, A. C., Luo, J. & Der, C. J. Drugging the undruggable RAS: Mission Possible? *Nat Rev Drug Discov* **13**, 828–851 (2014).
2. Canon, J. *et al.* The clinical KRAS(G12C) inhibitor AMG 510 drives anti-tumour immunity. *Nature* **575**, 217–223 (2019).
3. Ostrem, J. M., Peters, U., Sos, M. L., Wells, J. A. & Shokat, K. M. K-Ras(G12C) inhibitors allosterically control GTP affinity and effector interactions. *Nature* **503**, 548–551 (2013).
4. Hallin, J. *et al.* The KRASG12C Inhibitor MRTX849 Provides Insight toward Therapeutic Susceptibility of KRAS-Mutant Cancers in Mouse Models and Patients. *Cancer Discovery* **10**, 54–71 (2020).
5. Gehringer, M. & Laufer, S. A. Emerging and Re-Emerging Warheads for Targeted Covalent Inhibitors: Applications in Medicinal Chemistry and Chemical Biology. *J. Med. Chem.* **62**, 5673–5724 (2019).
6. Moore, A. R., Rosenberg, S. C., McCormick, F. & Malek, S. RAS-targeted therapies: is the undruggable drugged? *Nat Rev Drug Discov* **19**, 533–552 (2020).
7. Wang, H. *et al.* Annual review of KRAS inhibitors in 2022. *European Journal of Medicinal Chemistry* **249**, 115124 (2023).
8. Fell, J. B. *et al.* Identification of the Clinical Development Candidate **MRTX849** , a Covalent KRAS^{G12C} Inhibitor for the Treatment of Cancer. *J. Med. Chem.* **63**, 6679–6693 (2020).
9. Zhao, D., Liu, Y., Yi, F., Zhao, X. & Lu, K. Recent advances in the development of inhibitors targeting KRAS-G12C and its related pathways. *European Journal of Medicinal Chemistry* **259**, 115698 (2023).
10. Meyer Zu Vilsendorf, I., Einerhand, J., Mulac, D., Langer, K. & Lehr, M. 1-Benzylindoles as inhibitors of cytosolic phospholipase A_2 α: synthesis, biological activity, aqueous solubility, and cell permeability. *RSC Med. Chem.* **15**, 641–659 (2024).
11. Lanman, B. A. *et al.* Discovery of a Covalent Inhibitor of KRASG12C (AMG 510) for the Treatment of Solid Tumors. *J. Med. Chem.* **63**, 52–65 (2020).
12. Koch, P. D., Quintana, J., Ahmed, M. S., Kohler, R. H. & Weissleder, R. Small Molecule Imaging Agent for Mutant KRAS G12C. *Advanced Therapeutics* **4**, 2000290 (2021).
13. Xiao, X. *et al.* Design, synthesis and pharmacological evaluation of bicyclic and tetracyclic pyridopyrimidinone analogues as new KRASG12C inhibitors. *European Journal of Medicinal Chemistry* **213**, 113082 (2021).
14. Ostrem, J. M. L. & Shokat, K. M. Targeting KRAS G12C with Covalent Inhibitors. *Annu. Rev. Cancer Biol.* **6**, 49–64 (2022).
15. Gentile, D. R. *et al.* Ras Binder Induces a Modified Switch-II Pocket in GTP and GDP States. *Cell Chemical Biology* **24**, 1455-1466.e14 (2017).
16. Shang, Y. *et al.* Design, synthesis and biological evaluation of pyrrolopyrimidine urea derivatives as novel KRASG12C inhibitors for the treatment of cancer. *European Journal of Medicinal Chemistry* **289**, 117391 (2025).
17. Li, A. *et al.* Design, Structure Optimization, and Preclinical Characterization of JAB-21822, a Covalent Inhibitor of KRASG12C. *J. Med. Chem.* **68**, 2422–2436 (2025).